https://doi.org/10.5194/egusphere-2025-5063
Preprint. Discussion started: 6 November 2025

Identification of Dust-Dominated Periods and a $PM_{2.5}$ Correction Based Solely on Plantower PMS Sensor Observations

Kamaljeet Kaur[1], Tristalee Mangin[1], Kerry Kelly[1]

[1]Department of Chemical Engineering, University of Utah, Salt Lake City, UT, 84112, USA

Correspondence to: Kamaljeet Kaur(kamaljeet.kaur@chemeng.utah.edu)

Abstract. The Plantower PMS5003/6003 sensor is widely used for low-cost monitoring of particulate matter (PM), but it substantially underestimates $PM_{2.5}$ and PM_{10} during dust events. This limitation is especially critical in the arid regions, such as the western United States, where windblown dust frequently degrades air quality, visibility, and public health. Identification of dust episodes typically relies on federal reference or equivalent method (FRM/FEM) monitors, often supplemented with satellite or meteorological data, but these resources have limited spatial resolution. This study examines whether dust episodes can be directly identified from PMS5003 sensor outputs. We analyzed measurements from 109 PMS sensors collocated or nearby 75 U.S. EPA monitoring sites with hourly FEM $PM_{2.5}$ and/or PM_{10} between January 2017 to May 2025. Two dust-event cutoff thresholds (threshold1 and threshold2) were developed using the sensor-reported ratio of coarse (2.5–10 µm) to ultrafine (0.3–1 µm) mass concentration, and relative humidity, to identify potential dust events. The thresholds can be used in real time, relying on the preceding 336 hourly measurements (consistent with PurpleAir's public archive display). To improve $PM_{2.5}$ estimates from the PMS sensor (pm2.5_alt, a common correction for Plantower PMS measurements reported by PurpleAir), this study used pm2.5_alt measurements identified as potential dust events to develop a correction factor for dust events through non-linear regression. This correction reduced the mean bias error between pm2.5_alt and FEM $PM_{2.5}$ for 103 of the 109 sensors by 59.8 ± 24.3%, while ensuring that the mean bias error did not fall below -1 µg/m³. This framework enhances the utility of PMS5003/6003 sensors for detecting and quantifying dust-related pollution episodes, extending monitoring capabilities in regions where regulatory coverage is limited.

1 Introduction

Plantower particulate matter sensors (PMS) are among the most widely used low-cost sensors for measuring particulate matter (PM) in ambient and indoor air (Barkjohn et al., 2021; Jaffe et al., 2023; Kim et al., 2025; Searle et al., 2023; Wallace et al., 2022). The PurpleAir (PA) network uses PMS sensors, and as of August 12, 2025, it had deployed 26,055 nodes worldwide (Worldwide, Ranked Data by PurpleAir, 2025). Additionally, other sensor networks use PMS sensors (Air Quality Egg - Science is Collaboration, 2025; Outdoor Air Quality Monitor, 2025; Air Quality Monitoring. Monitor in UK & Europe. Airly Data Platform and Monitors | Airly, 2025; Low-Cost Air Quality Monitoring & Measurement | Clarity Movement Co., 2025; QuantAQ, 2025; TELLUS Air Quality Monitoring Data and Solutions, 2025). The PMS5003 found in the PA-II is one of the most commonly used $PM_{2.5}$ sensors; this sensor reports particle number concentrations in six size bins, along with PM_1 (PM with aerodynamic diameter less than 1 µm), $PM_{2.5}$ (PM with aerodynamic diameter less than 2.5 µm), PM_{10} (PM with aerodynamic diameter less than 10 µm), temperature (T), and relative humidity (RH) measurements (Barkjohn et al., 2021; Kaur and Kelly, 2023a; Sayahi et al., 2019; Searle et al., 2023). The PA-II typically contains two sensors per node, which provides an indication of measurement consistency (Barkjohn et al., 2021).

The PMS5003 sensor has been extensively studied, and numerous correction factors have been developed to improve its $PM_{2.5}$ measurement accuracy under varying environmental conditions (Ardon-Dryer et al., 2020; Barkjohn et al., 2021, 2022; Cowell et al., 2022; Hong et al., 2021; Hua et al., 2021; Jaffe et al., 2023; Kaur and Kelly, 2023b; Magi et al., 2020; Mai et al., 2025; Malings et al., 2020; Mathieu-Campbell et al., 2024; Nilson et al., 2022; Patel et al., 2024; Raheja et al., 2023; Si et al., 2020; Tryner et al., 2020b; Wallace, 2023; Wallace et al., 2022; Weissert et al., 2025). Some of the most commonly used correction algorithms, such as pm2.5_alt and Barkjohn's U.S. universal correction, can be integrated into PurpleAir's real-time maps (Barkjohn et al., 2021; Wallace, 2023). However, a persistent limitation of the PMS sensors is their inability to accurately detect larger particles (roughly >1 μm in diameter) (Gautam et al., 2025a; He et al., 2020; Kaur & Kelly, 2023a; Kosmopoulos et al., 2023; Kuula et al., 2020, Ouimette et al., 2022; Tryner, Mehaffy, et al., 2020), which leads to a significant underestimation of sensor-reported $PM_{2.5}$ and PM_{10} concentrations during dust events (Gautam et al., 2025b; Jaffe et al., 2023; Kaur and Kelly, 2023b; Masic et al., 2020; Vogt et al., 2021; Weissert et al., 2025). This significant underestimation of PM levels during dust events can be misleading. For example, looking at a map of $PM_{2.5}$ concentrations from a source that utilizes Plantower PMS sensors during a dust event will likely show inaccurately low PM concentrations, which can lead individuals and decision makers to significantly underestimate the associated health risks. Over the long term, this can lead to distrust in these low-cost sensor networks. Prior studies (Kuula et al., 2020; Ouimette et al., 2024; Ouimette et al., 2022) have demonstrated that this underestimation of coarse PM is due to scattering truncation error. This occurs because the photodiode in the sensor is poorly positioned to detect forward-scattered light, which is dominant for large particles, meaning the sensor often fails to register them effectively.

During dust events, PMS sensors tend to exhibit poor or inconsistent performance compared to federal reference (FRM) or equivalent method (FEM) measurements (Jaffe et al., 2023; Kaur and Kelly, 2023b; Weissert et al., 2025). Identifying dust events typically relies on FEM $PM_{2.5}$ and PM_{10} measurements to obtain an estimate of coarse PM, which can be supplemented by satellite imagery, chemical speciation, visibility reports, and high wind speed indicators (Hand et al., 2017; Jaffe et al., 2023; Kaur and Kelly, 2023b; Robinson and Ardon-Dryer, 2024; Sandhu et al., 2024; Tong et al., 2012). However, the availability of FEM, FRM, and other high-quality measurements is limited. For example, the continental United States has 2,141 $PM_{2.5}$ and 672 PM_{10} monitoring sites, respectively, with only 502 locations operating both $PM_{2.5}$ and PM_{10} monitors (AirNow-Tech: Home, 2025). In addition, satellite products are typically available after a time delay; for example, MODIS data is usually available 60 to 125 minutes after the satellite observation (MODIS Near Real-Time Data | NASA Earthdata, 2025). Thus, relying on FEM/FRM measurements or satellite products is impractical for large-scale or real-time applications (Brahney et al., 2024). To address these limitations, some studies have used nearby FEM sites to estimate correction factors for PMS sensors (Weissert et al., 2025). These methods often rely on rolling 3- or 4-day correlations or FEM-to-PMS concentration ratios, but such strategies have limitations, including limited spatial representativeness and time lags. Dust events typically last a few hours (Brahney et al., 2024). A rolling 3-or 4-day average cannot be applied in real time, and it may not accurately reflect the dust event because the correlation would include a dust event (i.e., time period dominated by coarse PM) and time periods dominated by other sources.

Recognizing dust events is particularly important in western regions of the United States, where such events occur frequently due to arid landscapes, land disturbance, sparse vegetation, and high wind activity. These regions, including parts of California, Arizona, Utah, New Mexico, and Texas, experience elevated levels of windblown dust, which can significantly impact air quality, visibility, and public health (Ardon-Dryer et al., 2023a, b; Goudie, 2014; Hahnenberger and Nicoll, 2012; Lei et al., 2016; Lewis et al., 2011; Robinson and Ardon-Dryer, 2024). Accurate detection and correction of dust-related pollution are therefore essential for both regulatory monitoring and public exposure assessments (Ardon-Dryer et al., 2023a).

This manuscript examines whether it is possible to identify a dust event solely based on measurements from a PMS sensor, without relying on external data sources such as FEM monitors, satellite imagery, or meteorological data. This question is inspired by findings from Ouimette et al. (2024), who noted that although the PMS sensor is often described as a nephelometer, it actually counts individual particles. In the PMS sensor, the probability of detection increases with particle size, meaning larger particles are more likely to be counted. However, the PMS does not effectively size the large particles (>1 µm) to the correct bin, due to scattering truncation errors. Correctly sizing these larger particles depends on their passage through the sensor's focal point, where sufficient light scattering occurs to be detected by the photodiode. Ouimette et al. (2024) estimated that the probability of a 10 µm particle being correctly sized in a PMS sensor to produce a detectable signal is less than 2%. Consequently, on days with relatively low PM levels, counts in the coarse particle bin (2.5–10 µm) are expected to be negligible due to both the scarcity of coarse particles and the low probability of correct bin assignment. During dust events, however, the particle size distribution shifts toward larger diameters, increasing the number of coarse particles. Even with the low probability of correct classification, the coarse bin registers higher counts compared to clean days, reflecting the increased presence of coarse particles and providing a potential pathway for identifying dust events using the sensor alone. Building on this rationale, Jaffe et al. (2023) proposed using the ratio of 0.3 µm to 5 µm PMS bin counts as a dust indicator, suggesting a cutoff value of 190, below which measurements were likely associated with dust events, and suggested a correction method using the measurements from one site, Keeler, California. Their method improved corrected PMS $PM_{2.5}$ measurements during dust events at this single controlled site (operated by the air quality agency), but it did not provide a useful correction for most of the 50 other sensors, collocated at monitoring stations (Jaffe et al., 2023).

Building on these previous studies (Jaffe et al., 2023; Ouimette et al., 2024), this study developed sensor-specific parameters for identifying potential dust events, derived solely from PMS sensor measurements, without relying on external data sources. By analyzing internal metrics, such as particle count distributions, RH, and T. It provides a framework that can be applied to any PMS5003 sensor, regardless of location, to identify potential dust events. This approach enhances the usability of the vast network of publicly available sensors for dust detection, even in areas where regulatory monitoring is lacking.

2 Method

This section describes the PMS sensor, the data sources, and the time periods used in this study. It also describes the PMS sensor data cleaning procedures, the sensor parameters of interest, the post-processing and real-time approaches for identifying potential dust events, correction methods for potential dust event measurements, and finally, the statistical tools used for data analysis.

2.1 Plantower PMS5003 and PMS6003 sensors

Several studies have described the Plantower PMS5003 sensors and their laboratory and field performance (Barkjohn et al., 2021, 2022; Ouimette et al., 2024; Ouimette et al., 2022; Sayahi et al., 2019). PMS5003 uses a fan to create flow (~1.67 mL/sec), a red laser (~680 +/- 10 nm), a scattering angle of 90º, and a photo-diode detector to measure total scattering from a plume of particles (Kaur & Kelly, 2023a; Ouimette et al., 2022). The sensor converts the total light scattering into several different air quality parameters, including particle counts in six bins (ranging between 0.3-10 µm), and PM_1, $PM_{2.5}$, and PM_{10} using an embedded algorithm. The flow path involves more than one 90-degree turn before particles reach the photodiode. Several other models of the Plantower PMS sensor exist (i.e., PMS1003, 3003, 6003, 7003, 9003, A003, T003, X003). Kaur and Kelly (2023a) evaluated the PMS6003 and found that the PMS5003 and PMS6003 exhibited similar performance to coarse PM. Many of the PMS models have similar configurations and likely exhibit similar challenges with accurately measuring coarse PM, although this has not been systematically evaluated.

This study used the PurpleAir network PMS sensors, i.e., PA-II. This study period began in 2017 and spanned several years, during which time the PA-II nodes came in different configurations (PA-II, PA-II-SD, and PA-II-FLEX), employed two different Plantower PMS sensors (PA-II and PA-II-SD: 5003 and PA-II-FLEX: 6003), and used different firmware versions (6.06b, 7.02, and 7.04). Due to the lack of detailed documentation on how different firmware

https://doi.org/10.5194/egusphere-2025-5063
Preprint. Discussion started: 6 November 2025

versions affected sensor performance, no firmware-based exclusions were made. The PA-II-SD model is a PA-II sensor variant that includes an SD card for data storage; both of these variations were included in the study. The PMS6003, used in PA-II-FLEX, differs from PMS5003, primarily in the number of lasers used (as described in Kaur and Kelly (2023a)), but its flow design, performance, and overall configuration are similar to the PMS5003 (Kaur and Kelly, 2023a). Accordingly, PA-II-FLEX data were not treated differently in this analysis. The ratio of >0.5 µm to 0.3 µm (ratio greater than 0.4) was used to identify the alternate PMS5003 (Searle et al., 2023), and none of the sensors used in the study were alternate PMS5003. For the remaining part of the manuscript, the sensors will be referred as PMS sensors.

2.2 Sensor selection, data access, and cleaning

This study evaluated 109 PMS sensors at 75 different US EPA monitoring sites with hourly FEM measurements of $PM_{2.5}$ and/or PM_{10}. The US EPA provided measurements from 28 of these 109 collocated sensors, which were previously used by Barkjohn et al. (2021). These 28 sensors are subset of the 50 sensors originally used in the Barkjohn paper because: 5 sensors were collocated with 24-hour averaged FRM measurements; 6 had less than 3 month of collocated measurements; 5 had poor correlation (R^2 less than 0.5, after removing the dust days using FEM based coarser fraction and PM_{10} concentrations); 2 were situated at beach; and 4 were already included in this study. Of the remaining 81 sensors, 77 were publicly available sensors and were downloaded (2-min frequency) using PurpleAir's Data Download Tool (v1.3.5), and 4 additional PMS5003s were available from the authors' group at the University of Utah. The publicly available sensors were considered collocated if the sensor had the same GPS coordinates (latitude and longitude) as the EPA monitoring site; if the sensor did not have the same coordinates but was within 0.8 km, the sensor was treated as a "nearby" sensor. Thirteen of the 77 sensors were "nearby" sensors, which increased spatial diversity by adding 13 additional monitoring sites. This study spanned from January 2017 to May 2025; however, data availability varied by sensor, depending on its deployment dates. The supplementary materials include sensor IDs, the corresponding collocated EPA monitoring site IDs, and each sensor's data availability (Tables S1, S2, S3) and a map with the 75 EPA monitoring sites used in this study (Figure S1).

The downloaded measurements included particle counts in the six size bins, RH, and pm2.5_alt. All the sensors used in this study had a minimum of three months of reasonably continuous data. The PMS measurements were cleaned, partially following guidelines by Barkjohn et al. (2022). Specifically, the 2-min averages were converted to hourly measurements if 27 or more 2-minute stamps existed in an hour (>90 % completion). Otherwise, the measurement was considered incomplete and not further analyzed. Next, the hourly measurements of dual nodes were considered valid if (a) the difference between the pm2.5_alt values for A and B nodes of PA was less than 5 µg/m^3, or (b) the relative percentage difference was less than 61%. Barkjohn et al. (2022) used pm2.5_cf_1, while this study used the pm2.5_alt to clean the PM measurements. We selected pm2.5_alt because pm2.5_cf_1 can exhibit random elevated values (order of 1000s) (Barkjohn et al., 2021), even when the number counts in the six bins are in a reasonable range. The pm2.5_alt is calculated directly from the bin counts (Wallace, 2023)and is less susceptible to random spikes. This study also used the PMS sensor's reported RH and T (using BME280, Bosch Sensortec, Germany) measurements. Therefore, PM measurements with missing RH and T were excluded from the study. This resulted in the removal of <5% of the measurement for 94 sensors, between 5 – 10 % for 7 sensors, between 10 – 22% for 6 sensors, and 34.7% and 64.9% for the CA15 and CO3 sensors.

2.3 FEM measurements

FEM measurements of $PM_{2.5}$ and PM_{10} were accessed from the AQS site (Download Files | AirData | US EPA, 2025) for the period between Jan 2017 – July 2024 (this data was unavailable after July 2024). For the remaining period,

https://doi.org/10.5194/egusphere-2025-5063
Preprint. Discussion started: 6 November 2025

i.e., between July 2024 – May 2025, the data was accessed through the AirNow API (AirNow API Documentation, 2025).

Most sites employed the beta attenuation and broadband spectroscopy method (i.e., Teledyne T640 and T640x) for Federal Equivalent Method (FEM) hourly $PM_{2.5}$ and PM_{10} measurements. A few sites also used FDMS (filter dynamic measurement system) in conjunction with a TEOM (tapered element oscillating microbalance) and laser light scattering (GRIMM) for hourly PM measurements. Table S1 and Table S2 detail the methods used for $PM_{2.5}$ and PM_{10} measurement at each site.

Some sites had multiple parameter occurrence codes (POCs), either from different measurement methods or from multiple instruments using the same method operating concurrently. For sites with two different methods active simultaneously, measurements from the method with the greater number of measurements was used. For sites equipped with the Teledyne T640X and Teledyne T640, this study used the POC corresponding to the EPA-corrected measurements (Regulations.gov, 2025).

When both FEM $PM_{2.5}$ and PM_{10} measurements were available, the coarse fraction (CF) was calculated as:

$$\mathrm{CF} = \frac{\mathrm{PM_{10}} - \mathrm{PM_{2.5}}}{\mathrm{PM_{10}}} \tag{1}$$

Where PM_{10} and $PM_{2.5}$ were concentrations in $\mu g/m^3$.

Dust typically has high CF values (>0.7) (Sugimoto et al., 2016). These CF values can help evaluate the effectiveness of our proposed method (discussed in section 2.5) in identifying times with a high proportion of coarse particles (i.e., potential dust events). Of the 109 sensors evaluated in this study, 30 sensors did not have CF data for their evaluation period, and 36 sensors had CF data for 90% of their evaluation period. A total of 35 sites had CF data for 40 – 90% of their evaluation period, and the remaining 8 sensors had CF data for less than 30% of their evaluation period.

2.4 Parameters

This study used the following parameters from the PMS sensors to identify potential dust events

1. Ratio of mass in the coarse fraction to ultrafine fraction (CF_to_UF): This ratio was defined as:

$$\mathrm{CF\_to\_UF} = \frac{\overline{\mathrm{M}_{2.5-5}} + \overline{\mathrm{M}_{5-10}}}{\overline{\mathrm{M}_{0.3-0.5}} + \overline{\mathrm{M}_{0.5-1}}} \tag{2}$$

Where $\mathrm{M_{i-j}}$ represents the mass concentration ($\mu g/m^3$) provided by the PMS sensor in the bin with size bin i – j µm. The $\overline{\mathrm{M_{i-j}}}$ is the average of valid $\mathrm{M_{i-j}}$ measurements from node A and node B of the PMS sensors. The $\mathrm{M_{i-j}}$, used here and previously by Wallace et al. (Wallace, 2023), was calculated as:

$$\mathrm{M_{i-j}} = \frac{4}{3}\pi\left(\frac{\sqrt{\mathrm{i*j}}}{2}\right)^3 * \mathrm{N_{i-j}} * 10^2 \tag{3}$$

The $\mathrm{N_{i-j}}$ represents the number counts of particles (#/dl) in the size bin i – j µm. The density was assumed to be 1 g/cm^3. The 10^2 accounts for the unit conversions in the equation (μm^3 to m^3; g/cm^3 to $\mu g/m^3$; and 1/dl to $1/m^3$).

The $\mathrm{CF_{to_{UF}}}$ parameter was used to identify dust events. This approach builds on the rationale presented in Ouimette et al. (2024) and discussed in the Introduction. Briefly, although coarse PM has a low probability of correct classification, the coarse bin will register elevated counts during dust events. Consequently, the CF_to_UF ratio becomes elevated during dust events.

https://doi.org/10.5194/egusphere-2025-5063
Preprint. Discussion started: 6 November 2025

2. RH: PMS sensor RH measurements are biased low by approximately 10 %–20 % (Mathieu-Campbell et al., 2024). This bias tended to increase at higher RH, although the PA's RH measurements generally show good correlation with regulatory RH measurements (R^2 >0.9) (Mathieu-Campbell et al., 2024). Dust events are typically associated with low RHs (< 40 – 60%) (Csavina et al., 2014), as higher humidity tends to inhibit dust suspension and promotes faster resettling of particles. We used an RH of 50%, as measured by the PMA sensor, as a threshold for detecting dust. It should be noted that an RH of 50% reported by the PMS sensor corresponds to an actual RH of ~70%. The cutoff of 50% is supported by Figure S2, which illustrates that elevated CF_to_UF with high CF was predominantly associated with RH less than 50%. This study explored dust event selection without the use of RH, and the results are discussed in the supplementary section S1.

2.5 Methods for identifying potential dust events

Our method included two approaches. The first focuses on post-processing the sensor measurements to identify potential dust events and to develop appropriate corrections for subsequent applications. The second approach emphasizes real-time identification of potential dust events. Both approaches use the parameters CF_to_UF and RH. The post-processing approach establishes the framework for real-time detection, as it provides a clearer way to illustrate the methodology. However, the same real-time approach could also be applied to post-processing the sensor data.

2.5.1 Post-processing approach

To identify potential dust events, two sensor-specific CF_to_UF based thresholds (threshold1 and threshold2) were defined using the full dataset for each sensor.

- Threshold1 was calculated as the sum of the median of CF_to_UF and a factor (F of 2.5) times the median absolute deviation (MAD) of the CF_to_UF.

$$\text{Threshold1} = \text{Median}(\text{CF\_to\_UF}) + F * \text{MAD}(\text{CF\_to\_UF}) \quad (4)$$

$$\text{MAD} = \text{Median}(|\text{CF\_to\_UF} - \text{Median}(\text{CF\_to\_UF})|) \quad (5)$$

- Threshold2 was defined as the maximum of:
  I. Three times the slope (with the intercept fixed at zero) from a linear regression of CF_to_UF (y-axis) against pm2.5_alt (x-axis), or
  II. A value of 0.584, i.e., three times the median slope of the slopes from all the sensors evaluated in this study.

Figure 1 displays Threshold1 and Threshold2 for a subset of representative sensors (for selected sites with a history of windblown dust impacts). Threshold1 was primarily used to differentiate clean days from those with elevated coarse particle concentrations. Because high coarse-concentration events typically occur under specific meteorological conditions (e.g., during dust events or wildfires), most measurements were expected to reflect low coarse PM concentrations. Consequently, most CF_to_UF values represent these low-coarse concentration conditions, and the overall median serves as a baseline CF_to_UF for such conditions. The outliers in the CF_to_UF would represent high coarse concentration measurements. To identify these outliers, we excluded the measurements near the baseline by setting a threshold, i.e., 2.5 times the MAD of the median. Previous studies have reported that F values of 3, 2.5, or 2 are effective for detecting outliers (Leys et al., 2013), with F = 3 considered conservative and F = 2.5 moderately conservative.

https://doi.org/10.5194/egusphere-2025-5063
Preprint. Discussion started: 6 November 2025

Threshold2 helped differentiate between potential dust events from other sources that may also increase CF_to_UF. For example, during wildfires both PM_{10} and $PM_{2.5}$ levels are typically elevated, which could lead to high CF_to_UF values, but also high pm2.5_alt concentrations. Threshold2, defined by the slope between pm2.5_alt and CF_to_UF (Figure 1), serves as a dynamic threshold to filter out high CF_to_UF values that are not associated with dust, specifically when both CF_to_UF and pm2.5_alt are high.

Threshold1 and threshold2 were calculated using all available measurements, irrespective of the availability of FEM $PM_{2.5}$ concentrations. A measurement was labeled as a potential dust event if:

- CF_to_UF exceeded threshold1, and
- CF_to_UF / pm2.5_alt exceeded threshold2, and
- RH from the PA measured less than 50 %,

As observed from Figure 1 and Figure S3, high CF_to_UF were observed at low pm2.5_alt values, and using threshold1 and threshold2, the identified measurements corresponded to high CF, as confirmed by the FEM based CF measurements.

2.5.2 Real-time detection of the dust events

For real-time potential dust event detection, threshold1 was defined as the median of CF_to_UF plus 2.5 times its MAD, calculated from the preceding 336 hourly measurements (14 days). Thus, threshold1 was dynamic. This 14-day window was selected to match the temporal coverage of the PA real-time map, which provides the most recent 14 days of hourly measurements.

Threshold2 was set at a fixed value of 0.584, from the measurements discussed in the post-processing approach (Section 2.5.1). This fixed threshold of 0.584 was selected to avoid using a slope calculated from just 336 points, which can be highly sensitive to outliers, as a few extreme values can distort the slope.

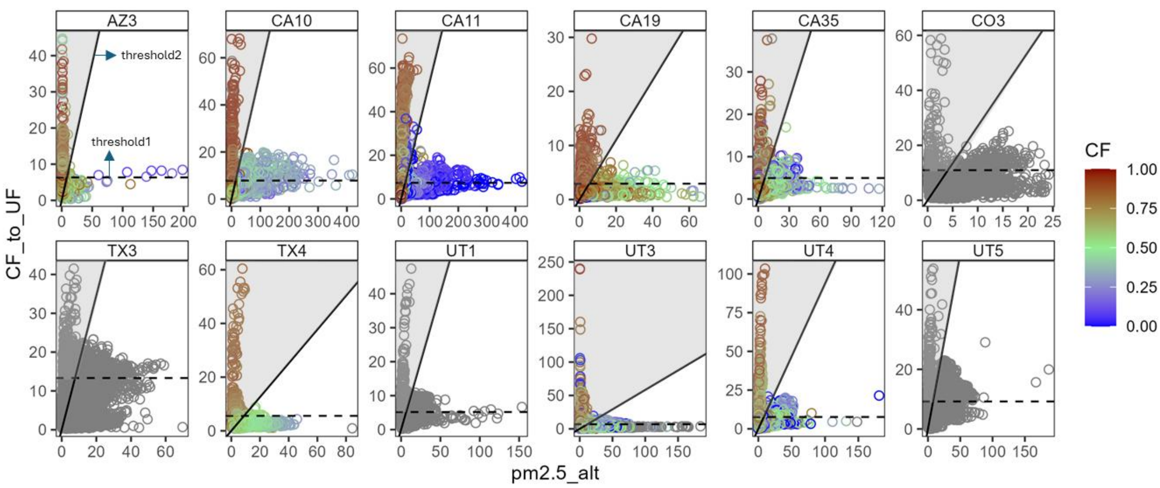

Figure 1: pm2.5_alt vs. CF_to_UF. Each point represents an hourly averaged sensor measurement, colored by the FEM-calculated CF. The black dashed line represents threshold1, and the black solid line represents threshold2. The shaded grey region indicates measurements identified as potential dust events. Solid grey circles represent times when

https://doi.org/10.5194/egusphere-2025-5063
Preprint. Discussion started: 6 November 2025

either $PM_{2.5}$ or PM_{10} was unavailable, preventing the calculation of CF. The comparison of pm2.5_alt vs. CF_to_UF for the remaining sensors is shown in Figure S3.

2.5.3 Correction of measurements identified as dust events

The pm2.5_alt concentration was adjusted (referred to as adj_pm2.5_alt) using a non-linear regression model that incorporated FEM $PM_{2.5}$, pm2.5_alt, CF_to_UF, threshold1, and a scaling factor A. Measurements identified as potential dust events based on threshold1, threshold2, and RH thresholds were combined across all sensors for the post-processing approach and real-time approach. These pooled dust-event measurements were then used to estimate factor A for each approach through non-linear regression, as follows:

$$\mathrm{adj}_{\mathrm{pm2.5}_{\mathrm{alt}}} \sim \mathrm{FEM\ PM}_{2.5} = \frac{\mathrm{CF\_to\_UF}}{\mathrm{threshold1} * \mathrm{A}} * \mathrm{pm2.5}_{\mathrm{alt}} \tag{6}$$

Factor A was calculated as 0.702 for the post-processing approach and 0.998 for the real-time approach. Only the measurements identified as potential dust events were adjusted, while all other measurements remained unchanged. The use of A of 0.702 to correct real-time approach identified measurements was also explored.

Threshold2 was not included in the correction equation because its sole purpose was to exclude non-dust events that produced elevated CF_to_UF values. In contrast, threshold1 was applied to normalize CF_to_UF values, enabling measurements from all sensors to be pooled together. This normalization ensured that the correction was not disproportionately influenced by sensors with high CF_to_UF values. By normalizing with threshold1, data from all sensors could be combined to derive a single factor (A = 0.702).

2.6 Analysis

Data analysis was performed using R (4.4.0). The primary focus of the analysis was to compare pm2.5_alt with FEM $PM_{2.5}$ concentrations, with an emphasis on potential dust events, and to evaluate the effectiveness of the applied correction approach. No additional corrections (i.e., adjustments for RH or FEM instrument calibration) were applied to pm2.5_alt. This study focused solely on the comparison between pm2.5_alt and FEM $PM_{2.5}$, and adj_pm2.5_alt and FEM $PM_{2.5}$. The performance of our correction approach was evaluated using the difference in the mean bias error (MBE, µg/m³) before and after correction of pm2.5_alt.

$$\mathrm{MBE} = \frac{1}{n}\sum_{i=1}^{n}\left(\mathrm{FEM\ PM2.5}_i - \mathrm{pm2.5}_{\mathrm{alt}_i}\right) \tag{7}$$

$$\mathrm{MBE}_{\mathrm{adj}} = \frac{1}{n}\sum_{i=1}^{n}\left(\mathrm{FEM\ PM2.5}_i - \mathrm{adj}_{\mathrm{pm2.5}_{\mathrm{alt}_i}}\right) \tag{8}$$

MBE was calculated only for those measurements identified as potential dust events. The remaining measurements were not corrected and not included in the MBE calculation. In the main manuscript, we present results for selected locations that have collocated measurements and are affected by windblown dust, including sites in Utah, Arizona, Texas, Colorado, and California. The results for the remaining locations are discussed in the supplementary material.

3 Results and discussion

3.1 Measurement identified as potential dust event using the thresholds

Table S4 summarizes the counts of the threshold-based identification of potential dust events, which identified 0 – 3785 (post-processing approach: 0 – 9.00 %) and 0 – 4513 (real-time approach: 0 – 9.62 %) hourly averaged

https://doi.org/10.5194/egusphere-2025-5063
Preprint. Discussion started: 6 November 2025

measurements as potential dust events. These counts did not consider the availability of FEM $PM_{2.5}$ measurements. The real-time approach generally identified more measurements than the post-processing approach (Figure S4, Table S4). This outcome was expected because the real-time method used a dynamic threshold1, whereas the post-processing method used a constant threshold1. A dynamic threshold1 accommodates shifts in the CF_to_UF baseline (defined in Section 2.5.1), which can occur when a sensor operates for extended periods (example in Figure S5) or when a PMS sensor is replaced within a node (example in Figure S5), resulting in CF_to_UF baseline shifts due to differences in sensor-specific performance characteristics.

Seasonal variability in CF_to_UF further complicates the use of a constant threshold1 (example in Figure S4). When most measurements originate from seasons with elevated PM concentrations, the overall threshold1 was biased upward, leading to the rejection of high-coarse concentration measurements during seasons with lower CF_to_UF values. The reverse holds when measurements were dominated by low-concentration seasons. In contrast, the dynamic threshold1 adjusts for these seasonal shifts, thereby improving measurement selection (Figure S5).

Figure S6 compares the PMS measurements identified as potential dust events to the CF of PM, which was grouped into the following CF bins (0–0.25, 0.25–0.5, 0.5–0.7, and >0.7). The majority of potential dust event measurements were associated with the CF > 0.7 bin (67.1 ± 23.4% for the post-processing approach and 70.2 ± 20.8% for the real-time approach), followed by the bin between 0.5 and 0.7 (18.9 ± 17.1% and 19.2 ± 15.9%, respectively). Fewer than 8.50% of measurements fell within the 0.25–0.5 bin, and fewer than 5.50% fell within the 0–0.25 bin. This distribution, with most measurements in CF > 0.7, supported the thresholds applied in this study for identifying dust events. The CF between 0.5 and 0.7 could represent dust mixed with other sources.

3.2 $PM_{2.5}$ vs. pm2.5_alt: post-processing approach

Figure 2 (top) illustrates the measurements, identified as potential dust events, for 12 representative sites. These measurements corresponded predominantly to cases in which pm2.5_alt underestimated FEM $PM_{2.5}$, typically associated with CF > 0.7. Figure 2 (bottom) illustrates the same measurements after adjustment using the correction equation developed in this study. Comparisons of pm2.5_alt and FEM $PM_{2.5}$ for the remaining sites were presented in Figures S7 and S8.

https://doi.org/10.5194/egusphere-2025-5063
Preprint. Discussion started: 6 November 2025

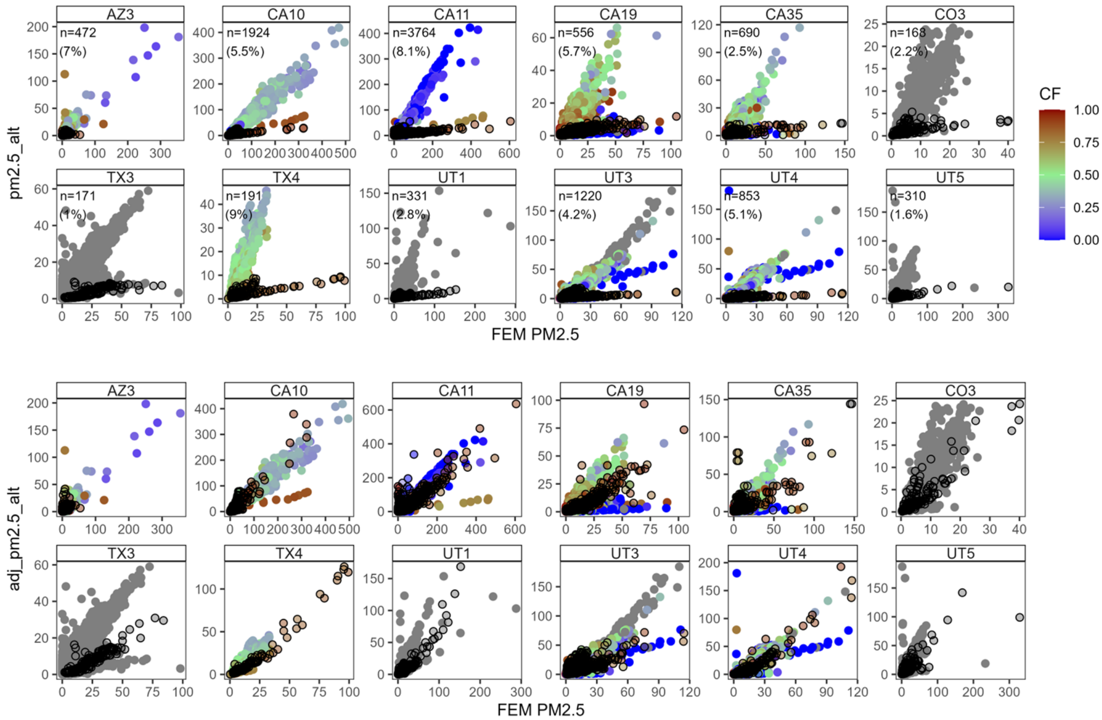

Figure 2: Post-processing approach: (top) Hourly averaged pm2.5_alt compared with FEM $PM_{2.5}$ measurements. Black open circles indicate measurements identified as dust events. (bottom) Hourly averaged adj_pm2.5_alt compared with FEM $PM_{2.5}$ measurements. The color of the solid circles corresponds to the CF. The grey solid circles represent times when either $PM_{2.5}$ or PM_{10} was unavailable, preventing the calculation of CF. n denotes the number of measurements identified as potential dust events, for a subset of data when FEM $PM_{2.5}$ data were available. Table S4 shows the total number of dust-event measurements, regardless of FEM $PM_{2.5}$ availability. Comparisons of pm2.5_alt and FEM $PM_{2.5}$ for the remaining sites were presented in Figures S7 and S8.

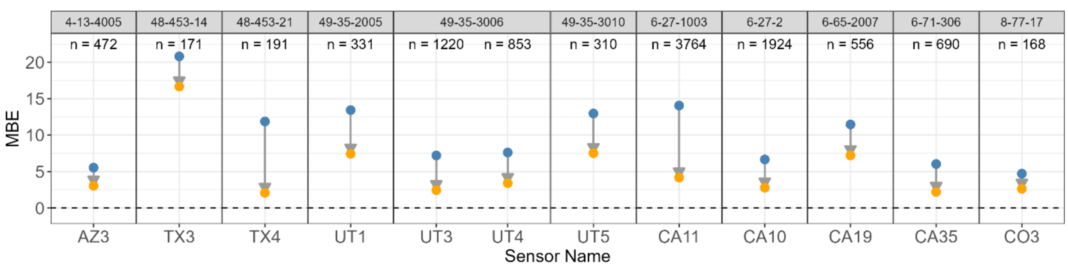

Figure 3: Post-processing approach: change in MBE with respect to FEM $PM_{2.5}$ before and after adjusting pm2.5_alt. The blue dot represents the MBE before correction, while the orange dot represents the MBE after correction. The grey arrow highlights the direction of the MBE shift after correction. n represents the number of potential dust event measurements. The lower x-axis corresponds to the sensor name, while the top x-axis corresponds to the site where these sensors were located. Comparisons of MBE and MBE_adj for the remaining sites were presented in Figure S9.

https://doi.org/10.5194/egusphere-2025-5063
Preprint. Discussion started: 6 November 2025

Figure 3 presents MBE and MBE_adj. An MBE value closer to zero indicates better sensor performance, meaning that the sensor-estimated $PM_{2.5}$ concentrations are more consistent with the FEM $PM_{2.5}$ measurements. For the 12 sensors shown in the main manuscript, MBE decreased by 52.4 ± 16.9% on average, with MBE ranging between 4.71 – 20.81 µg/m^3 and MBE_adj ranging between 2.07 – 16.7 µg/m^3. The MBE_adj remained positive, indicating that although the sensor's $PM_{2.5}$ estimation has improved, it remained less than FEM $PM_{2.5}$ after correction.

For the remaining sensors (Figure S9 and Table S4), 82 sensors had MBE that decreased from 1.54 – 14.60 µg/m^3 to MBE_adj of -0.76 – 7.60 µg/m^3, i.e., a decrease of 49.6 ± 22.9 %. For 13 sensors, the MBE_adj was less than -1 µg/m^3, indicating the correction led to overestimation of the $PM_{2.5}$ concentrations. For two sensors, no measurements were identified as potential dust events. Among the sensors with negative MBE_adj (Figure S9), 7 had fewer than 60 measurements (<0.6%) identified as potential dust events and belonged to states of AK, IA, OR, WA, and VT. The locations of these monitors are not frequently affected by dust. Even for sensors with negative MBE_adj, the adjusted pm2.5_alt concentration remained within the sensor's expected range (Figure S8).

It is important to note that the locations of most sensors were identified based on the PA public map, and no physical verification of collocation was available, except for 4 sensors maintained by the authors' group and the sensor list provided by the EPA. Given this uncertainty, some variability in MBE outcomes was expected.

3.3 Real-time processing: pm2.5_alt vs. FEM $PM_{2.5}$

Figure 4 (top) illustrates the measurements identified as potential dust events for 12 representative sites using the real-time approach. Figure 4 (bottom) illustrates the same measurements after adjustment using the correction equation developed in this study. Figure 5 shows MBE and MBE_adj.

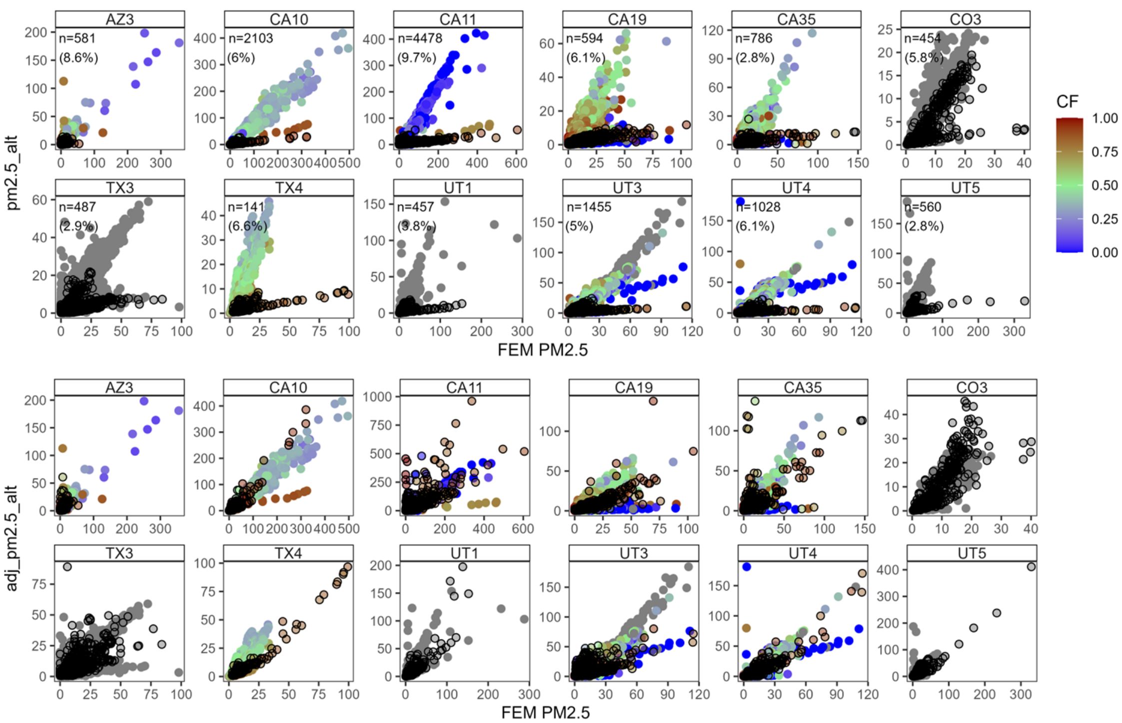

https://doi.org/10.5194/egusphere-2025-5063
Preprint. Discussion started: 6 November 2025

Figure 4: Real-time approach: (top) Hourly averaged pm2.5_alt values compared to FEM $PM_{2.5}$ measurements. (bottom) Hourly averaged adj_pm2.5_alt, adjusted using A of 0.702, compared with FEM $PM_{2.5}$ measurements. The color of the solid circles corresponds to the CF. The grey solid circles represent times when either $PM_{2.5}$ or PM_{10} was unavailable, preventing the calculation of CF. n denotes the number of measurements identified as potential dust events, for a subset of data when FEM $PM_{2.5}$ data were available. Black open circles represent measurements identified as potential dust events. Comparisons of pm2.5_alt and FEM $PM_{2.5}$ for the remaining sites were presented in Figure S10.

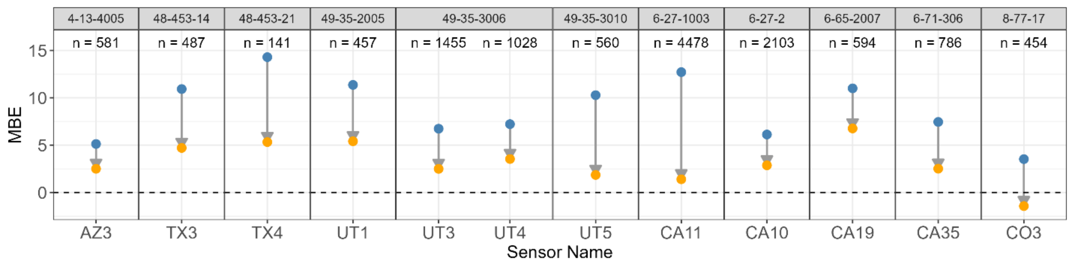

Figure 5: Real-time approach: change in MBE with respect to FEM $PM_{2.5}$ before and after adjusting pm2.5_alt using A of 0.702. The blue dot represents the MBE before correction, while the orange dot represents the MBE after correction. The grey arrow highlights the direction of MBE shift after correction. n represents the number of potential dust event measurements. The lower x-axis corresponds to the sensor name, while the top x-axis corresponds to the site where these sensors were located. Comparisons of MBE and MBE_adj for the remaining sites were presented in Figure S11.

Out of the 12 sensors, shown in the manuscript, 11 sensors' MBE_adj decreased (from 5.12 – 14.3 µg/m^3 to 1.39 – 6.76 µg/m^3, a change of 60.6 ± 14.5 %) but remained positive (Figure 5). The CO3 sensor MBE declined from 3.52 µg/m^3 to -1.44 µg/m^3, indicating the A of 0.702 resulted in the CO3 adj_pm2.5_alt to be higher than FEM $PM_{2.5}$. If using the A of 0.998 (obtained using the real-time approach identified potential dust events), all 12 sensor MBE_adj remained positive, but the decrease in the MBE was low (34.5 +/- 11.1%) (Figure S12).

Across the remaining sensors (Figure S11 and Table S4), using A of 0.702, most sensors also showed improvement; for 89 sensors MBE dropped from 0.713 – 14.4 to MBE_adj of -0.622 – 7.58 µg/m^3, a change of 59.7 ± 21.2 %). Two sensors did not have any events identified as potential dust events (Table S4). A smaller subset (5 sensors) exhibited MBE_adj of less than -1 µg/m^3, with MBE_adj values ranging from -3.63 – -1.16 µg/m^3 (Figure S11 and Table S4). One notable outlier, sensor WA3, showed a larger negative MBE_adj (-8.77 µg/m^3); however, this sensor had only 33 measurements identified as potential dust events. The use of A of 0.998 (Figure S12), resulted in MBE_adj between -0.613 – 10.48 µg/m^3, a decrease of 28.4 ±23.9 % for all sensors, with the exception of WA3 (MBE_adj of -4.06 µg/m^3, a decrease of 212.9%). The factor A in the correction equation determined the extent of the pm2.5_alt adjustment.

The correction of pm2.5_alt measurements (adj_pm2.5_alt) in this study was driven by a single adjustment factor, A, which directly influenced MBE. A constant value of A was applied to all sensors to maintain generalizability and ensure the approach could be deployed in real time across a geographically broad network of PMS sensors. While this strategy provided a practical solution, it was not equally effective for all sensors, likely because each site experiences different PM compositions and each sensor has unique performance characteristics.

To explore the potential benefit of individual calibration, sensor-specific values of A were tested for potential dust events using the real-time approach (Figure S13). With sensor-specific A, for all sensors, the MBE dropped from 0.713 – 14.4 to -0.497 – 9.40, i.e., a reduction of 53.2 ± 31.2 %. These results demonstrate that sensor-specific calibration can substantially improve accuracy. However, implementing sensor-specific A requires calibration against a reference instrument before deployment, ideally under a range of PM concentrations and compositions representative of the

https://doi.org/10.5194/egusphere-2025-5063
Preprint. Discussion started: 6 November 2025

target environment. This requirement limits scalability and may not be feasible for geographically diverse networks. Thus, there is a trade-off: a fixed A offers simplicity and consistency for a broad distribution of sensors, while a sensor-specific A improves accuracy but reduces generality. In future work, integrating sensor-specific calibration during initial deployment may offer a balanced solution, improving accuracy while maintaining some level of practicality for network-scale monitoring.

4 Limitations

This study has several limitations, primarily related to the use of PMS sensors and the assumptions made in selecting and interpreting the data. First, most PMS sensors used in this analysis were identified from the publicly available PA map, and their physical locations and deployment conditions could not be independently confirmed. It is possible that some of the sensors selected were not truly collocated with the FEM instruments. Second, PA nodes are user-deployed and can be moved or reconfigured at any time. A user might relocate the entire sensor, swap sensor nodes, or even replace hardware without any indication in the metadata. Such changes can alter sensor performance or the environmental context of the measurements (e.g., from outdoor to indoor), potentially affecting CF_to_UF values and the thresholds used for dust event detection. These untracked changes may lead to inconsistencies in the correction approach, either causing genuine dust events to be missed or non-dust days to be mistakenly corrected due to a sudden shift in sensor behavior. Additionally, the correction method depends on long-term consistency in sensor performance. Any drift in sensor response (deSouza et al., 2023), contamination of the sensor inlet, changes in the PMS production process (i.e., (Searle et al., 2023)), or firmware updates may also influence measurement characteristics and correction effectiveness. A potential limitation of this approach is that it may be less effective under consistently high-dust conditions, as the baseline correction assumes that the environment is relatively clean most of the time. Finally, this study evaluated PMS5003/6003s, and the proposed methods would need to be evaluated for other PMS models. Despite these limitations, the general trends and methodology proposed in this manuscript can provide a useful framework for real-time and retrospective identification of possible dust events using PMS sensors. However, future work should aim to validate sensor-reference collocation and investigate the impact of node-level changes on the robustness of corrections.

Some potentially problematic measurements were not explicitly excluded in this study. These included: (i) periods with all zero counts in bins >0.5 µm throughout the sampling duration; (ii) spurious temperature readings (e.g., ~ –129 °F) persisting over the study period; and (iii) inconsistent particle count assignments, such as higher counts in the >0.5 µm bin compared to the >0.3 µm bin, or in the >2.5 µm bin compared to the >5 µm bin, which sometimes resulted in negative pm2.5_alt concentrations. While the thresholds developed in this study may have excluded many of these problematic data points, they may also have inadvertently excluded valid dust events.

5 Future Work

Our approach for identifying elevated coarse particle concentrations could be extended to improve PM_{10} estimation from low-cost sensors. Furthermore, in conjunction with back-trajectory models, meteorological data, or satellite imagery, this method could help identify the sources of PM_{10} plumes, such as dust sources, construction activity, or agricultural emissions. In addition, if A could be defined for each sensor based on laboratory calibration under controlled conditions, it could significantly enhance the accuracy of real-time dust event detection and correction. This could enhance both the scalability and robustness of using low-cost sensors, such as the PMS, for dust monitoring in diverse environmental settings.

https://doi.org/10.5194/egusphere-2025-5063
Preprint. Discussion started: 6 November 2025

6 Conclusion

This study demonstrates that PMS5003/6003 sensors, despite their well-known limitations in detecting coarse particles, can be used to identify and provide reasonably accurate $PM_{2.5}$ measurements during dust events using only sensor's reported outputs. By leveraging particle counts in the coarser and ultrafine bin and RH, we developed real-time thresholds (threshold1 and threshold2) that successfully identified dust episodes without reliance on external datasets. Between 0 and 3785 hourly averaged $PM_{2.5}$ measurements (0–9.00%) from each sensor were identified as potential dust events with the post-processing approach, and 0–4513 measurements (0–9.62%) with the real-time approach. The real-time method consistently identified more dust episodes, owing to its dynamic threshold1, which better accounted for seasonal and sensor-specific variability. Most identified potential dust events were associated with coarse fraction values >0.7 (67–70%) as measured by FEMs, confirming that the thresholds targeted conditions when PMS sensors most strongly underestimated FEM $PM_{2.5}$. Correction of PMS $PM_{2.5}$ estimates (pm2.5_alt) substantially reduced bias. For the 12 sensors highlighted in this manuscript, MBE decreased by ~52% (MBE: 4.71 – 20.8 $\mu g/m^3$; MBE_adj: 2.07 – 16.7 $\mu g/m^3$) with the post-processing approach and 60% (MBE: 3.52 – 14.3 μg/m3; MBE_adj: -1.44 – 6.76 $\mu g/m^3$) with the real-time approach. Across the broader dataset, 82 sensors improved under post-processing (MBE: 1.54 – 14.6 $\mu g/m^3$; MBE_adj: -0.760 to 7.60 $\mu g/m^3$) and 89 sensors improved under real-time adjustment (MBE: 0.713 – 14.4 $\mu g/m^3$; MBE_adj: -0.622 to 7.58 $\mu g/m^3$). Only a small subset (13 for post-processing and 6 for real-time processing) showed less than -1 $\mu g/m^3$ MBE_adj, often at sites that infrequently experience dust events or with very few flagged dust events (<0.7% of measurements). Overall, the framework developed here improves PMS5003 performance during potential dust events, reduces $PM_{2.5}$ underestimation, and extends the utility of low-cost sensors for dust monitoring in regions with sparse FRM/FEM coverage.

7 Acknowledgement

Research reported in this publication is based upon work supported by the National Science Foundation under grant no. 2012091 (Collaborative Research Network Cluster: Dust in the Critical Zone) and under grant no. 2322009 (CIVIC-Stage2: TRACK A: Community Resilience through Engaging, Actionable, Timely, High-Resolution Air Quality Information – CREATE-AQI). The authors wish to thank Dr. Karoline Barkjohn (US EPA) for the valuable feedback on the manuscript and for providing a collocation dataset of PA sensors and regulatory monitors. This EPA collocation dataset would not have been possible without the partnership of many air monitoring agencies and other partners, including the State of Alaska, Citizens for Clean Air (Alaska), Maricopa County Air Quality Department, San Luis Obispo County Air Pollution Control District, Mojave Desert Air Quality Management District, California Air Resources Board, Santa Barbara County Air Pollution Control District, Ventura County Air Pollution Control District, South Coast Air Quality Management District and its Air Quality Sensor Performance Evaluation Center (AQ-SPEC), Colorado Department of Public Health and Environment, Delaware Division of Air Quality, Sarasota County Government, Georgia Environmental Protection Division, Iowa Department of Natural Resources, Kansas Department of Health and Environment, Missoula County, Montana Department of Environmental Quality, Forsyth County Office of Environmental Assistance and Protection, Clean Air Carolina, Quapaw Nation, Oklahoma Department of Environmental Quality, Virginia Department of Environmental Quality, State of Vermont, Puget Sound Clean Air Agency, and Wisconsin Department of Natural Resources. Thanks to PurpleAir for allowing access to their data at no cost. AI-assisted tools were used to edit the original drafts of the manuscript to enhance the clarity and readability of the text.

8 Conflict of interest

Kerry E. Kelly has a financial interest in the company Tellus Networked Solutions, LCC, which commercializes solutions for environmental monitoring. Their technology was not used as part of this work.

https://doi.org/10.5194/egusphere-2025-5063
Preprint. Discussion started: 6 November 2025

9 References

Air Quality Egg: *Air Quality Egg - Science is Collaboration*. https://airqualityegg.com/home, last access: 09 August 2025.

AirGradient: *Outdoor Air Quality Monitor*. https://www.airgradient.com/outdoor/, last access: 09 August 2025.

Airly: *Air Quality Monitoring. Monitor in UK & Europe. Airly Data Platform and Monitors | Airly*. https://airly.org/en/, last access: 09 August 2025.

AirNow Data Management Center: *AirNow-Tech: Home*. https://www.airnowtech.org/, last access: 09 August 2025.

Ardon-Dryer, K., Clifford, K. R., & Hand, J. L. (2023). Dust Under the Radar: Rethinking How to Evaluate the Impacts of Dust Events on Air Quality in the United States. *GeoHealth*, *7*(12), e2023GH000953. https://doi.org/10.1029/2023GH000953

Ardon-Dryer, K., Dryer, Y., Williams, J. N., & Moghimi, N. (2020). Measurements of PM2.5 with PurpleAir under atmospheric conditions. *Atmospheric Measurement Techniques*, *13*(10), 5441–5458. https://doi.org/10.5194/AMT-13-5441-2020,

Ardon-Dryer, K., Gill, T. E., & Tong, D. Q. (2023). When a Dust Storm Is Not a Dust Storm: Reliability of Dust Records From the Storm Events Database and Implications for Geohealth Applications. *GeoHealth*, *7*(1). https://doi.org/10.1029/2022GH000699

Barkjohn, K. K., Gantt, B., & Clements, A. L. (2021). Development and application of a United States-wide correction for PM2.5 data collected with the PurpleAir sensor. *Atmospheric Measurement Techniques*, *14*(6), 4617–4637. https://doi.org/10.5194/AMT-14-4617-2021,

Barkjohn, K. K., Holder, A. L., Frederick, S. G., & Clements, A. L. (2022). Correction and Accuracy of PurpleAir PM2.5 Measurements for Extreme Wildfire Smoke. *Sensors*, *22*(24), 9669. https://doi.org/10.3390/S22249669/S1

Brahney, J., Heindel, R. C., Gill, T. E., Carling, G., González-Olalla, J. M., Hand, J., Mallia, D. V., Munroe, J. S., Perry, K., Putman, A. L., Skiles, S. M., Adams, B. R., Aanderud, Z., Aarons, S., Aguirre, D., Ardon-Dryer, K., Blakowski, M. B., Creamean, J. M., Fernandez, D., … Merrill, T. (2024). Dust in the Critical Zone: North American case studies. *Earth-Science Reviews*, *258*, 104942. https://doi.org/10.1016/J.EARSCIREV.2024.104942

Clarity: *Low-Cost Air Quality Monitoring & Measurement | Clarity Movement Co.* https://www.clarity.io/, last access: 09 August 2025.

Cowell, N., Chapman, L., Bloss, W., & Pope, F. (2022). Field Calibration and Evaluation of an Internet-of-Things-Based Particulate Matter Sensor. *Frontiers in Environmental Science*, *9*, 798485. https://doi.org/10.3389/FENVS.2021.798485/BIBTEX

Csavina, J., Field, J., Félix, O., Corral-Avitia, A. Y., Sáez, A. E., & Betterton, E. A. (2014). Effect of wind speed and relative humidity on atmospheric dust concentrations in semi-arid climates. *Science of The Total Environment*, *487*(1), 82–90. https://doi.org/10.1016/J.SCITOTENV.2014.03.138

deSouza, P., Barkjohn, K., Clements, A., Lee, J., Kahn, R., Crawford, B., & Kinney, P. (2023). An analysis of degradation in low-cost particulate matter sensors. *Environmental Science: Atmospheres*, *3*(3), 521–536. https://doi.org/10.1039/D2EA00142J

https://doi.org/10.5194/egusphere-2025-5063
Preprint. Discussion started: 6 November 2025

EPA: *Regulations.gov*. https://www.regulations.gov/document/EPA-HQ-OAR-2023-0642-0031, last access: 09 August 2025.

EPA: *Download Files | AirData | US EPA*. https://aqs.epa.gov/aqsweb/airdata/download_files.html, last access: 09 August 2025.

EPA AirNow Data Management Center: *AirNow API Documentation*. https://docs.airnowapi.org/, last access: 09 August 2025.

Gautam, P., Ramirez, A., Bair, S., Arnott, W. P., Chow, J. C., Watson, J. G., Moosmüller, H., & Wang, X. (2025a). Sizing Accuracy of Low-Cost Optical Particle Sensors Under Controlled Laboratory Conditions. *Atmosphere*, *16*(5), 502. https://doi.org/10.3390/ATMOS16050502/S1

Gautam, P., Ramirez, A., Bair, S., Arnott, W. P., Chow, J. C., Watson, J. G., Moosmüller, H., & Wang, X. (2025b). Sizing Accuracy of Low-Cost Optical Particle Sensors Under Controlled Laboratory Conditions. *Atmosphere*, *16*(5), 502. https://doi.org/10.3390/ATMOS16050502/S1

Goudie, A. S. (2014). Desert dust and human health disorders. *Environment International*, *63*, 101–113. https://doi.org/10.1016/J.ENVINT.2013.10.011

Hahnenberger, M., & Nicoll, K. (2012). Meteorological characteristics of dust storm events in the eastern Great Basin of Utah, U.S.A. *Atmospheric Environment*, *60*, 601–612. https://doi.org/10.1016/J.ATMOSENV.2012.06.029

Hand, J. L., Gill, T. E., & Schichtel, B. A. (2017). Spatial and seasonal variability in fine mineral dust and coarse aerosol mass at remote sites across the United States. *Journal of Geophysical Research: Atmospheres*, *122*(5), 3080–3097. https://doi.org/10.1002/2016JD026290

He, M., Kuerbanjiang, N., & Dhaniyala, S. (2020). Performance characteristics of the low-cost Plantower PMS optical sensor. *Aerosol Science and Technology*, *54*(2), 232–241. https://doi.org/10.1080/02786826.2019.1696015

Hong, G. H., Le, T. C., Tu, J. W., Wang, C., Chang, S. C., Yu, J. Y., Lin, G. Y., Aggarwal, S. G., & Tsai, C. J. (2021). Long-term evaluation and calibration of three types of low-cost PM2.5 sensors at different air quality monitoring stations. *Journal of Aerosol Science*, *157*, 105829. https://doi.org/10.1016/J.JAEROSCI.2021.105829

Hua, J., Zhang, Y., de Foy, B., Mei, X., Shang, J., Zhang, Y., Sulaymon, I. D., & Zhou, D. (2021). Improved PM2.5 concentration estimates from low-cost sensors using calibration models categorized by relative humidity. *Aerosol Science and Technology*, *55*(5), 600–613. https://doi.org/10.1080/02786826.2021.1873911;CTYPE:STRING:JOURNAL

Jaffe, D. A., Miller, C., Thompson, K., Finley, B., Nelson, M., Ouimette, J., & Andrews, E. (2023). An evaluation of the U.S. EPA's correction equation for PurpleAir sensor data in smoke, dust, and wintertime urban pollution events. *Atmospheric Measurement Techniques*, *16*(5), 1311–1322. https://doi.org/10.5194/AMT-16-1311-2023,

Kaur, K., & Kelly, K. E. (2023a). Laboratory evaluation of the Alphasense OPC-N3, and the Plantower PMS5003 and PMS6003 sensors. *Journal of Aerosol Science*, *171*, 106181. https://doi.org/10.1016/J.JAEROSCI.2023.106181

Kaur, K., & Kelly, K. E. (2023b). Performance evaluation of the Alphasense OPC-N3 and Plantower PMS5003 sensor in measuring dust events in the Salt Lake Valley, Utah. *Atmospheric Measurement Techniques*, *16*(10), 2455–2470. https://doi.org/10.5194/AMT-16-2455-2023, Kelley, M. C., & Ardon-Dryer, K. (2021). Analyzing two decades of dust events on the Southern Great Plains region of West Texas. *Atmospheric Pollution Research*, *12*(6), 101091. https://doi.org/10.1016/J.APR.2021.101091

Kim, K. T., Kim, H., Jeong, S., Lee, Y. S., Zhao, X., & Kim, J. Y. (2025). Coincidence effect of a low-cost particulate matter sensor: Observations from environmental chamber tests at diverse particle concentrations. *Atmospheric Pollution Research*, *16*(9), 102581. https://doi.org/10.1016/j.apr.2025.102581

Kosmopoulos, G., Salamalikis, V., Wilbert, S., Zarzalejo, L. F., Hanrieder, N., Karatzas, S., & Kazantzidis, A. (2023). Investigating the Sensitivity of Low-Cost Sensors in Measuring Particle Number Concentrations across Diverse Atmospheric Conditions in Greece and Spain, *Sensors 23(14), 6541*. https://doi.org/10.3390/s23146541

Kuula, J., Mäkelä, T., Aurela, M., Teinilä, K., Varjonen, S., González, Ó., & Timonen, H. (2020). Laboratory evaluation of particle-size selectivity of optical low-cost particulate matter sensors. *Atmospheric Measurement Techniques*, *13*(5), 2413–2423. https://doi.org/10.5194/AMT-13-2413-2020,

Lei, H., Wang, J. X. L., Tong, D. Q., & Lee, P. (2016). Merged dust climatology in Phoenix, Arizona based on satellite and station data. *Climate Dynamics*, *47*(9–10), 2785–2799. https://doi.org/10.1007/S00382-016-2997-7/METRICS

Lewis, J. M., Kaplan, M. L., Vellore, R., Rabin, R. M., Hallett, J., & Cohn, S. A. (2011). Dust storm over the Black Rock Desert: Larger-scale dynamic signatures. *Journal of Geophysical Research Atmospheres*, *116*(6). https://doi.org/10.1029/2010JD014784

Leys, C., Ley, C., Klein, O., Bernard, P., & Licata, L. (2013). Detecting outliers: Do not use standard deviation around the mean, use absolute deviation around the median. *Journal of Experimental Social Psychology*, *49*(4), 764–766. https://doi.org/10.1016/J.JESP.2013.03.013

Magi, B. I., Cupini, C., Francis, J., Green, M., & Hauser, C. (2020). Evaluation of PM2.5 measured in an urban setting using a low-cost optical particle counter and a Federal Equivalent Method Beta Attenuation Monitor. *Aerosol Science and Technology*, *54*(2), 147–159. https://doi.org/10.1080/02786826.2019.1619915;SUBPAGE:STRING:FULL

Mai, C., Wang, Z., Chen, L., Huang, Y., Li, M., Shirazi, A., Altaee, A., & Zhou, J. L. (2025). Field-based calibration and operation of low-cost sensors for particulate matter by linear and nonlinear methods. *Atmospheric Pollution Research*, *16*(12), 102676. https://doi.org/10.1016/J.APR.2025.102676

Malings, C., Tanzer, R., Hauryliuk, A., Saha, P. K., Robinson, A. L., Presto, A. A., & Subramanian, R. (2020). Fine particle mass monitoring with low-cost sensors: Corrections and long-term performance evaluation. *Aerosol Science and Technology*, *54*(2), 160–174. https://doi.org/10.1080/02786826.2019.1623863

Masic, A., Bibic, D., Pikula, B., Blazevic, A., Huremovic, J., & Zero, S. (2020). Evaluation of optical particulate matter sensors under realistic conditions of strong and mild urban pollution. *Atmospheric Measurement Techniques*, *13*(12), 6427–6443. https://doi.org/10.5194/AMT-13-6427-2020,

Mathieu-Campbell, M. E., Guo, C., Grieshop, A. P., & Richmond-Bryant, J. (2024). Calibration of PurpleAir low-cost particulate matter sensors: model development for air quality under high relative humidity conditions. *Atmospheric Measurement Techniques*, *17*(22), 6735–6749. https://doi.org/10.5194/amt-17-6735-2024

NASA Earthdata: *MODIS Near Real-Time Data | NASA Earthdata*. https://www.earthdata.nasa.gov/data/instruments/modis/near-real-time-data, last access: 09 August 2025.

https://doi.org/10.5194/egusphere-2025-5063
Preprint. Discussion started: 6 November 2025

Nilson, B., Jackson, P. L., Schiller, C. L., & Parsons, M. T. (2022). Development and evaluation of correction models for a low-cost fine particulate matter monitor. *Atmospheric Measurement Techniques*, *15*(11), 3315–3328. https://doi.org/10.5194/AMT-15-3315-2022,

Ouimette, J., Arnott, W. P., Laven, P., Whitwell, R., Radhakrishnan, N., Dhaniyala, S., Sandink, M., Tryner, J., & Volckens, J. (2024). Fundamentals of low-cost aerosol sensor design and operation. *Aerosol Science and Technology*, *58*(1), 1–15. https://doi.org/10.1080/02786826.2023.2285935

Ouimette, J. R., Malm, W. C., Schichtel, B. A., Sheridan, P. J., Andrews, E., Ogren, J. A., & Arnott, W. P. (2022). Evaluating the PurpleAir monitor as an aerosol light scattering instrument. *Atmospheric Measurement Techniques*, *15*(3), 655–676. https://doi.org/10.5194/amt-15-655-2022

Patel, M. Y., Vannucci, P. F., Kim, J., Berelson, W. M., & Cohen, R. C. (2024). Towards a hygroscopic growth calibration for low-cost PM2.5 sensors. *Atmospheric Measurement Techniques*, *17*(3), 1051–1060. https://doi.org/10.5194/AMT-17-1051-2024,

PurpleAir: *Worldwide, Ranked Data by PurpleAir*. https://location.purpleair.com/countries?layers=us_epa_aqi%2Caire_y_salud%2Caustralian_aqi%2Cbrazilian_pm25%2Caqhi_plus%2Cchinese_aqi%2Ceuropean_aqi%2Cindia_naqi%2Cindonesia_ispu%2Cnew_south_wales_pm_2_5%2Ctasmania_pm_2_5%2Cuk_daily_aqi%2Cc, last access: 09 August 2025.

QuantAQ: *QuantAQ*. https://quant-aq.com/, last access: 09 August 2025.

Raheja, G., Nimo, J., Appoh, E. K. E., Essien, B., Sunu, M., Nyante, J., Amegah, M., Quansah, R., Arku, R. E., Penn, S. L., Giordano, M. R., Zheng, Z., Jack, D., Chillrud, S., Amegah, K., Subramanian, R., Pinder, R., Appah-Sampong, E., Tetteh, E. N., … Westervelt, D. M. (2023). Low-Cost Sensor Performance Intercomparison, Correction Factor Development, and 2+ Years of Ambient PM2.5 Monitoring in Accra, Ghana. *Environmental Science and Technology*, *57*(29), 10708–10720. https://doi.org/10.1021/ACS.EST.2C09264/ASSET/IMAGES/LARGE/ES2C09264_0009.JPEG

Robinson, M. C., & Ardon-Dryer, K. (2024). Characterization of 21 years of dust events across four West Texas regions. *Aeolian Research*, *67–69*, 100930. https://doi.org/10.1016/J.AEOLIA.2024.100930

Sandhu, T., Robinson, M. C., Rawlins, E., & Ardon-Dryer, K. (2024). Identification of dust events in the greater Phoenix area. *Atmospheric Pollution Research*, *15*(11), 102275. https://doi.org/10.1016/J.APR.2024.102275

Sayahi, T., Butterfield, A., & Kelly, K. E. (2019). Long-term field evaluation of the Plantower PMS low-cost particulate matter sensors. *Environmental Pollution*, *245*, 932–940. https://doi.org/10.1016/J.ENVPOL.2018.11.065

Searle, N., Kaur, K., & Kelly, K. (2023). Technical note: Identifying a performance change in the Plantower PMS 5003 particulate matter sensor. *Journal of Aerosol Science*, *174*, 106256. https://doi.org/10.1016/J.JAEROSCI.2023.106256

Si, M., Xiong, Y., Du, S., & Du, K. (2020). Evaluation and calibration of a low-cost particle sensor in ambient conditions using machine-learning methods. *Atmospheric Measurement Techniques*, *13*(4), 1693–1707. https://doi.org/10.5194/AMT-13-1693-2020,

Sugimoto, N., Shimizu, A., Matsui, I., & Nishikawa, M. (2016). A method for estimating the fraction of mineral dust in particulate matter using PM2.5-to-PM10 ratios. *Particuology*, *28*, 114–120. https://doi.org/10.1016/J.PARTIC.2015.09.005

https://doi.org/10.5194/egusphere-2025-5063
Preprint. Discussion started: 6 November 2025

Tellus: *TELLUS Air Quality Monitoring Data and Solutions*. https://www.tellusensors.com/?utm_term=air%20quality%20sensor&utm_campaign=%2A%2ALP%20Search%20-%20Device&utm_source=adwords&utm_medium=ppc&hsa_acc=4349704448&hsa_cam=21839194498&hsa_grp=170850629202&hsa_ad=718136201884&hsa_src=g&hsa_tgt=aud-2266742649017%3Akwd-297848703289&hsa_kw=air%20quality%20sensor&hsa_mt=p&hsa_net=adwords&hsa_ver=3&gad_source=1&gad_campaignid=21839194498&gbraid=0AAAAAotNhB5506-Pvvvw6nag3jJ37RFy9&gclid=CjwKCAjw_fnFBhB0EiwAH_MfZsOaSkaCFNg7XJaW72ZOGdgJrqCvhANenfUngolN6dIKmj8KU9WiHxoCgmsQAvD_BwE, last access: 09 August 2025.

Tong, D. Q., Dan, M., Wang, T., & Lee, P. (2012). Long-term dust climatology in the western United States reconstructed from routine aerosol ground monitoring. *Atmos. Chem. Phys*, *12*, 5189–5205. https://doi.org/10.5194/acp-12-5189-2012

Tryner, J., L'Orange, C., Mehaffy, J., Miller-Lionberg, D., Hofstetter, J. C., Wilson, A., & Volckens, J. (2020). Laboratory evaluation of low-cost PurpleAir PM monitors and in-field correction using co-located portable filter samplers. *Atmospheric Environment*, *220*, 117067. https://doi.org/10.1016/J.ATMOSENV.2019.117067

Tryner, J., Mehaffy, J., Miller-Lionberg, D., & Volckens, J. (2020). Effects of aerosol type and simulated aging on performance of low-cost PM sensors. *Journal of Aerosol Science*, *150*, 105654. https://doi.org/10.1016/J.JAEROSCI.2020.105654

Tse, J., & Liang, L. (2025). Evaluating PurpleAir Sensors: Do They Accurately Reflect Ambient Air Temperature? *Sensors*, *25*(10), 3044. https://doi.org/10.3390/S25103044/S1

Vogt, M., Schneider, P., Castell, N., & Hamer, P. (2021). Assessment of Low-Cost Particulate Matter Sensor Systems against Optical and Gravimetric Methods in a Field Co-Location in Norway. *Atmosphere 2021, Vol. 12, Page 961*, *12*(8), 961. https://doi.org/10.3390/ATMOS12080961

Wallace, L. (2023). Cracking the code—Matching a proprietary algorithm for a low-cost sensor measuring PM1 and PM2.5. *Science of The Total Environment*, *893*, 164874. https://doi.org/10.1016/J.SCITOTENV.2023.164874

Wallace, L., Zhao, T., & Klepeis, N. E. (2022). Calibration of PurpleAir PA-I and PA-II Monitors Using Daily Mean PM2.5 Concentrations Measured in California, Washington, and Oregon from 2017 to 2021. *Sensors*, *22*(13), 4741. https://doi.org/10.3390/S22134741/S1

Weissert, L. F., Henshaw, G. S., Clements, A. L., Duvall, R. M., & Croghan, C. (2025). Seasonal effects in the application of the MOment MAtching (MOMA) remote calibration tool to outdoor PM2.5 air sensors. *Atmospheric Measurement Techniques*, *18*(15), 3635–3645. https://doi.org/10.5194/AMT-18-3635-2025,